

Improved Direct Measurement of the Parity-Violation Parameter A_b Using a Mass Tag and Momentum-Weighted Track Charge

Kenji Abe,¹⁵ Koya Abe,²⁴ T. Abe,²¹ I. Adam,²¹ H. Akimoto,²¹ D. Aston,²¹ K. G. Baird,¹¹ C. Baltay,³⁰ H. R. Band,²⁹ T. L. Barklow,²¹ J. M. Bauer,¹² G. Bellodi,¹⁷ R. Berger,²¹ G. Blaylock,¹¹ J. R. Bogart,²¹ G. R. Bower,²¹ J. E. Brau,¹⁶ M. Breidenbach,²¹ W. M. Bugg,²³ D. Burke,²¹ T. H. Burnett,²⁸ P. N. Burrows,¹⁷ A. Calcaterra,⁸ R. Cassell,²¹ A. Chou,²¹ H. O. Cohn,²³ J. A. Coller,⁴ M. R. Convery,²¹ V. Cook,²⁸ R. F. Cowan,¹³ G. Crawford,²¹ C. J. S. Damerell,¹⁹ M. Daoudi,²¹ N. de Groot,² R. de Sangro,⁸ D. N. Dong,²¹ M. Doser,²¹ R. Dubois,²¹ I. Erofeeva,¹⁴ V. Eschenburg,¹² S. Fahey,⁵ D. Falciari,⁸ J. P. Fernandez,²⁶ K. Flood,¹¹ R. Frey,¹⁶ E. L. Hart,²³ K. Hasuko,²⁴ S. S. Hertzbach,¹¹ M. E. Huffer,²¹ X. Huynh,²¹ M. Iwasaki,¹⁶ D. J. Jackson,¹⁹ P. Jacques,²⁰ J. A. Jaros,²¹ Z. Y. Jiang,²¹ A. S. Johnson,²¹ J. R. Johnson,²⁹ R. Kajikawa,¹⁵ M. Kalelkar,²⁰ H. J. Kang,²⁰ R. R. Kofler,¹¹ R. S. Kroeger,¹² M. Langston,¹⁶ D. W. G. Leith,²¹ V. Lia,¹³ C. Lin,¹¹ G. Mancinelli,²⁰ S. Manly,³⁰ G. Mantovani,¹⁸ T. W. Markiewicz,²¹ T. Maruyama,²¹ A. K. McKemey,³ R. Messner,²¹ K. C. Moffeit,²¹ T. B. Moore,³⁰ M. Morii,²¹ D. Muller,²¹ V. Murzin,¹⁴ S. Narita,²⁴ U. Nauenberg,⁵ H. Neal,³⁰ G. Nesom,¹⁷ N. Oishi,¹⁵ D. Onoprienko,²³ L. S. Osborne,¹³ R. S. Panvini,²⁷ C. H. Park,²² I. Peruzzi,⁸ M. Piccolo,⁸ L. Piemontese,⁷ R. J. Plano,²⁰ R. Prepost,²⁹ C. Y. Prescott,²¹ B. N. Ratcliff,²¹ J. Reidy,¹² P. L. Reinertsen,²⁶ L. S. Rochester,²¹ P. C. Rowson,²¹ J. J. Russell,²¹ O. H. Saxton,²¹ T. Schalk,²⁶ B. A. Schumm,²⁶ J. Schwiening,²¹ V. V. Serbo,²¹ G. Shapiro,¹⁰ N. B. Sinev,¹⁶ J. A. Snyder,³⁰ H. Staengle,⁶ A. Stahl,²¹ P. Stamer,²⁰ H. Steiner,¹⁰ D. Su,²¹ F. Suekane,²⁴ A. Sugiyama,¹⁵ S. Suzuki,¹⁵ M. Swartz,⁹ F. E. Taylor,¹³ J. Thom,²¹ E. Torrence,¹³ T. Usher,²¹ J. Va'vra,²¹ R. Verdier,¹³ D. L. Wagner,⁵ A. P. Waite,²¹ S. Walston,¹⁶ A. W. Weidemann,²³ E. R. Weiss,²⁸ J. S. Whitaker,⁴ S. H. Williams,²¹ S. Willocq,¹¹ R. J. Wilson,⁶ W. J. Wisniewski,²¹ J. L. Wittlin,¹¹ M. Woods,²¹ T. R. Wright,²⁹ R. K. Yamamoto,¹³ J. Yashima,²⁴ S. J. Yellin,²⁵ C. C. Young,²¹ and H. Yuta¹

(SLD Collaboration)

¹Aomori University, Aomori, 030 Japan

²University of Bristol, Bristol, United Kingdom

³Brunel University, Uxbridge, Middlesex UB8 3PH, United Kingdom

⁴Boston University, Boston, Massachusetts 02215

⁵University of Colorado, Boulder, Colorado 80309

⁶Colorado State University, Ft. Collins, Colorado 80523

⁷INFN Sezione di Ferrara and Universita di Ferrara, I-44100 Ferrara, Italy

⁸INFN Laboratori Nazionali di Frascati, I-00044 Frascati, Italy

⁹Johns Hopkins University, Baltimore, Maryland 21218-2686

¹⁰Lawrence Berkeley Laboratory, University of California, Berkeley, California 94720

¹¹University of Massachusetts, Amherst, Massachusetts 01003

¹²University of Mississippi, University, Mississippi 38677

¹³Massachusetts Institute of Technology, Cambridge, Massachusetts 02139

¹⁴Institute of Nuclear Physics, Moscow State University, 119899, Moscow Russia

¹⁵Nagoya University, Chikusa-ku, Nagoya, 464 Japan

¹⁶University of Oregon, Eugene, Oregon 97403

¹⁷Oxford University, Oxford OX1 3RH, United Kingdom,

¹⁸INFN Sezione di Perugia and Universita di Perugia, I-06100 Perugia, Italy

¹⁹Rutherford Appleton Laboratory, Chilton, Didcot, Oxon OX11 0QX United Kingdom

²⁰Rutgers University, Piscataway, New Jersey 08855

²¹Stanford Linear Accelerator Center, Stanford University, Stanford, California 94309

²²Soongsil University, Seoul, Korea 156-743

²³University of Tennessee, Knoxville, Tennessee 37996

²⁴Tohoku University, Sendai 980, Japan

²⁵University of California at Santa Barbara, Santa Barbara, California 93106

²⁶University of California at Santa Cruz, Santa Cruz, California 95064

²⁷Vanderbilt University, Nashville, Tennessee 37235

²⁸University of Washington, Seattle, Washington 98105

²⁹University of Wisconsin, Madison, Wisconsin 53706

³⁰Yale University, New Haven, Connecticut 06511

(Received 29 August 2002; published 10 April 2003)

We present an improved direct measurement of the parity-violation parameter A_b in the Z boson– b -quark coupling using a self-calibrating track-charge technique applied to a sample enriched in $Z \rightarrow b\bar{b}$ events via the topological reconstruction of the B hadron mass. Manipulation of the Stanford Linear Collider electron-beam polarization permits the measurement of A_b to be made independently of other Z -pole coupling parameters. From the 1996–1998 sample of 400 000 hadronic Z decays, produced with an average beam polarization of 73.4%, we find $A_b = 0.906 \pm 0.022(\text{stat}) \pm 0.023(\text{syst})$.

DOI: 10.1103/PhysRevLett.90.141804

PACS numbers: 13.38.Dg, 11.30.Er, 12.15.Ji, 14.65.Fy

Measurements of b -quark production asymmetries at the Z^0 pole determine the extent of parity violation in the $Zb\bar{b}$ coupling. At the Born level, the differential cross section for the process $e^+e^- \rightarrow Z^0 \rightarrow b\bar{b}$ can be expressed as a function of the polar angle θ of the b quark relative to the electron-beam direction,

$$\sigma^b(\cos\theta) \equiv d\sigma_b/d\cos\theta \propto (1 - A_e P_e)(1 + \cos^2\theta) + 2A_b(A_e - P_e)\cos\theta, \quad (1)$$

where P_e is the longitudinal polarization of the electron beam ($P_e > 0$ for a predominantly right-handed polarized beam). The parameter $A_f = 2v_f a_f / (v_f^2 + a_f^2)$, where v_f (a_f) is the vector (axial vector) coupling of the fermion f to the Z^0 boson, with $f = e$ or b , expresses the extent of parity violation in the $Zf\bar{f}$ coupling.

From the conventional forward-backward asymmetries formed with an unpolarized electron beam ($P_e = 0$), such as that used by the CERN Large Electron-Positron Collider (LEP) experiments, only the product $A_e A_b$ of parity-violation parameters can be measured [1]. With a longitudinally polarized electron beam, however, it is possible to measure A_b independently of A_e by fitting simultaneously to the differential cross sections of Eq. (1) formed separately for predominantly left- and right-handed beams. The resulting direct measurement of A_b is largely independent of propagator effects that modify the effective weak mixing angle and thus is complementary to other electroweak asymmetry measurements performed at the Z^0 pole.

In this Letter, we present a measurement of A_b based on the use of an inclusive vertex mass tag (improved relative to that of previous publications due to the use of an upgraded vertex detector) to select $Z \rightarrow b\bar{b}$ events and the net momentum-weighted track charge [2] to identify the charge of the underlying quark. This result, incorporating data collected during the 1996–1998 runs of the Stanford Linear Collider (SLC), is over twice as precise as that of our previous publication [3], which was based on data from 1993–1995.

The operation of the SLC with a polarized electron beam has been described elsewhere [4]. During the 1996–1998 run, the SLC Large Detector (SLD) [5] recorded an integrated luminosity of 14.0 pb^{-1} , at a mean center-of-mass energy of 91.24 GeV, and with a luminosity-weighted mean electron-beam polarization of $|P_e| =$

0.734 ± 0.004 [6]. The 1996–1998 run of the SLD detector incorporated the upgraded VXD3 CCD pixel vertex detector [7], which featured a greater coverage in $\cos\theta$, as well as a larger outer radius and substantially less material per layer, than that of the VXD2 vertex detector [8] in place from 1993–1995.

The SLD measures charged particle tracks with the Central Drift Chamber (CDC), which is immersed in a uniform axial magnetic field of 0.6 T. The VXD3 vertex detector provides an accurate measure of particle trajectories close to the beam axis. For the 1996–1998 data, the combined $r\phi$ (rz) impact parameter resolution of the CDC and VXD3 is 7.7 (9.6) μm at high momentum, and 34 (34) μm at $p_\perp \sqrt{\sin\theta} = 1 \text{ GeV}/c$, where p_\perp is the momentum transverse to the beam direction, and r (z) is the coordinate perpendicular (parallel) to the beam axis. The combined momentum resolution in the plane perpendicular to the beam axis is $\delta p_\perp / p_\perp = \sqrt{[(0.01)^2 + (0.0026 p_\perp / \text{GeV}/c)^2]}$. The thrust axis is reconstructed using the liquid argon calorimeter, which covers the angular range $|\cos\theta| < 0.98$.

The details of the analysis procedure are similar to those of the 1993–1995 sample analysis. Events are classified as hadronic Z^0 decays if they (i) contain at least seven well-measured tracks (as described in Ref. [5]); (ii) exhibit a visible charged energy of at least 20 GeV; and (iii) have a thrust axis polar angle satisfying $|\cos\theta_{\text{thrust}}| < 0.7$. The resulting hadronic sample from the 1996–1998 data consists of 245 048 events with a nonhadronic background estimated to be $< 0.1\%$.

We select against multijet events in order to reduce the dependence of the measured value of A_b on the effects of gluon radiation and interhemisphere correlation. Events are discarded if they are found to have four or more jets by the JADE jet-finding algorithm with $y_{\text{cut}} = 0.02$ [9], using reconstructed charged tracks as input. In addition, any event found to have three or more jets with $y_{\text{cut}} = 0.1$ is discarded.

To increase the $Z^0 \rightarrow b\bar{b}$ content of the sample, a tagging procedure based on the invariant mass of 3-dimensional topologically reconstructed secondary decay vertices is applied [10]. The mass of the reconstructed vertex is corrected for missing transverse momentum relative to the reconstructed B hadron flight direction in order to partially account for neutral particles. The requirement that the event contain at least one secondary vertex with mass greater than $2 \text{ GeV}/c^2$ results in a

sample of 36 936 candidate $Z^0 \rightarrow b\bar{b}$ decays. The purity (97%) and efficiency (77%) of this sample are calculated from the data by comparing the rates for finding a high mass vertex in either a single or both hemispheres, where the two hemispheres are defined relative to the plane perpendicular to the thrust axis. This procedure assumes *a priori* knowledge of the small $udsc$ tagging efficiency, as well as the size of interhemisphere correlations, both of which are taken from Monte Carlo (MC) simulation. This procedure also assumes knowledge of the $Z \rightarrow c\bar{c}$ and $Z \rightarrow b\bar{b}$ branching fractions, which are assigned their standard model values of 0.172 and 0.216, respectively.

We construct a signed thrust axis \hat{T} , which provides an estimate of the direction of the negatively charged b quark, as follows. Using all track-charge quality tracks, as defined in Ref. [11], we form the track-direction-signed (Q) and unsigned (Q_+) momentum-weighted track-charge sums

$$Q = - \sum_{\text{tracks}} q_j \cdot \text{sgn}(\vec{p}_j \cdot \hat{T}) |(\vec{p}_j \cdot \hat{T})|^\kappa, \quad (2)$$

$$Q_+ = \sum_{\text{tracks}} q_j |(\vec{p}_j \cdot \hat{T})|^\kappa, \quad (3)$$

where q_j and \vec{p}_j are the charge and momentum of track j , respectively. \hat{T} is chosen as the unit vector parallel to the thrust axis that renders $Q > 0$. We use $\kappa = 0.5$ to maximize the analyzing power of the track-charge algorithm for $Z^0 \rightarrow b\bar{b}$ events, resulting in a correct-assignment probability of 70%. Figure 1 shows the $T_z = \cos\theta_{\text{thrust}}$ distribution of the b -enriched sample separately for left- and right-handed electron beams. Clear forward-backward asymmetries are observed, with respective signs as expected from the cross-section formula in Eq. (1).

The value of A_b is extracted via a maximum likelihood fit to the differential cross section [see Eq. (1)]

$$p^i(A_b) = (1 - A_e P_e^i) [1 + (T_z^i)^2] + 2(A_e - P_e^i) T_z^i [A_b f_b^i (2p_b^i - 1)(1 - \Delta_{\text{QCD},b}^i) + A_c f_c^i (2p_c^i - 1)(1 - \Delta_{\text{QCD},c}^i) + A_{bckg} (1 - f_b^i - f_c^i) (2p_{bckg}^i - 1)], \quad (4)$$

where P_e^i is the signed polarization of the electron beam for event i , $f_{b(c)}^i$ is the probability that the event is a $Z^0 \rightarrow b\bar{b}(c\bar{c})$ decay (parametrized as a function of the secondary vertex mass), and $\Delta_{\text{QCD},b,c}^i$ are final-state QCD corrections, to be discussed below. A_{bckg} is the estimated asymmetry of residual $u\bar{u}$, $d\bar{d}$, and $s\bar{s}$ final states. The parameters p are estimates of the probability that the sign of Q accurately reflects the charge of the respective

underlying quark, and are functions of $|Q|$, as well as the secondary vertex mass and $|T_z|$.

As in our previous publication [3], we measure p_b directly from the data [12]. Defining Q_b ($Q_{\bar{b}}$) to be the track-direction-unsigned momentum-weighted track-charge sum for the thrust hemisphere containing the b (\bar{b}) quark, the quantities

$$Q_{\text{sum}} = Q_b + Q_{\bar{b}}, \quad Q_{\text{dif}} = Q_b - Q_{\bar{b}}, \quad (5)$$

may be related to the experimental observables defined in Eqs. (2) and (3), respectively: $|Q_{\text{dif}}| = |Q|$ and $Q_{\text{sum}} = Q_+$. Our MC simulation indicates that the Q_b and $Q_{\bar{b}}$ distributions are approximately Gaussian. In this limit [12],

$$p_b(|Q|) = \frac{1}{1 + e^{-\alpha_b |Q|}}, \quad (6)$$

with

$$\alpha_b = \frac{2q_{\text{dif}}^0}{\sigma_{\text{dif}}^2} = \frac{2\sqrt{\langle |Q_{\text{dif}}|^2 \rangle - \sigma_{\text{dif}}^2}}{\sigma_{\text{dif}}^2}, \quad (7)$$

where q_{dif}^0 and σ_{dif} are the mean and width, respectively, of the Gaussian Q_{dif} distribution. The parameter α_b , whose magnitude depends upon the separation between the b and \bar{b} track-sum distributions via the observable $\langle |Q_{\text{dif}}|^2 \rangle$, provides a measure of the analyzing power of the b -quark direction estimator \hat{T} . Figure 2 compares the distributions of the observable combinations $|Q_{\text{dif}}|$ and Q_+ between data and MC.

In the absence of a correlation between Q_b and $Q_{\bar{b}}$, $\sigma_{\text{dif}} = \sigma_{\text{sum}}$, where σ_{sum} is the observed width of the Q_+ distribution. Thus α_b can be derived from experimental

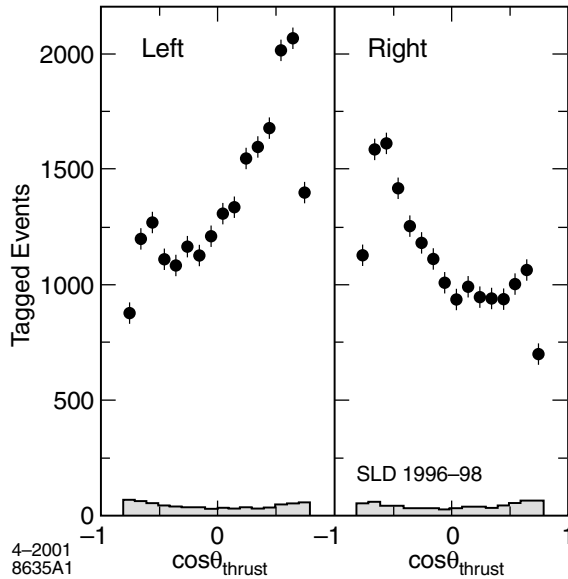


FIG. 1. Polar angle distributions for track-charge-signed $Z \rightarrow b\bar{b}$ candidates, separately for left- and right-handed electron beams. The shaded histogram represents the contribution from a non- $b\bar{b}$ background, estimated as described in the text. The analysis employs a cut of $|\cos\theta| < 0.7$.

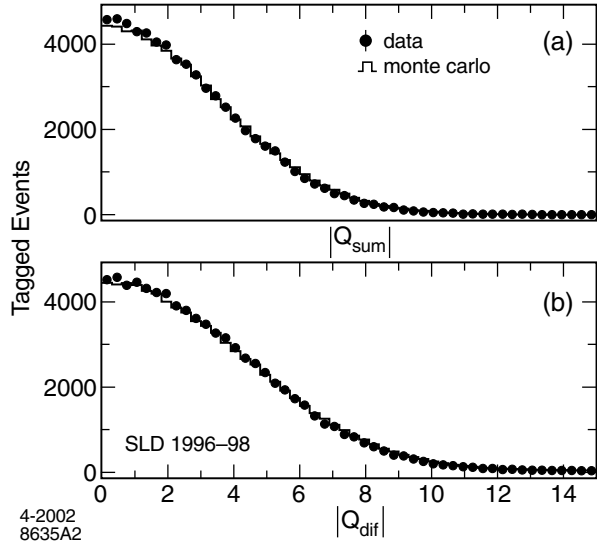


FIG. 2. Comparison between data (points) and MC (histogram) for the observables $|Q_{\text{sum}}|$ and $|Q_{\text{dif}}|$ (see text), for $Z \rightarrow b\bar{b}$ candidates.

observables. In the presence of a correlation, $\sigma_{\text{dif}} = (1 + \lambda)\sigma_{\text{sum}}$, where λ characterizes the strength of the correlation, which can be determined from the MC simulation. For JETSET 7.4 [13] with parton shower evolution, string fragmentation, and full detector simulation, λ is found to be 0.040. The effects of light-flavor contamination are taken into account by adjusting the observed widths σ_{sum}^2 and $\langle |Q_{\text{dif}}|^2 \rangle$, using the magnitude and width of the light-flavor and $c\bar{c}$ contributions estimated from the MC. This correction increases the value of α_b by 2% to 0.2944 ± 0.0078 , bringing it into good agreement with the value of 0.2949 ± 0.0007 extracted from the $Z \rightarrow b\bar{b}$ simulation.

Final-state gluon radiation reduces the observed asymmetry from its Born-level value. This effect is incorporated in our analysis by applying a correction $\Delta_{\text{QCD}}(|\cos\theta|)$ to the likelihood function [Eq. (4)]. Calculation of the quantity Δ_{QCD} has been performed by several groups [14].

For an unbiased sample of $b\bar{b}$ events, correcting for final-state gluon radiation increases the measured asymmetry by $\sim 3\%$. However, QCD radiative effects are mitigated by the use of the thrust axis to estimate the b -quark direction, the $Z^0 \rightarrow b\bar{b}$ enrichment algorithm, the self-calibration procedure, and the cut on the number of jets. A MC simulation of the analysis chain indicates that these effects can be represented by a $\cos\theta$ -independent suppression factor, $x_{\text{QCD}} = 0.074$, such that $\Delta_{\text{QCD}} = x_{\text{QCD}}\Delta_{\text{QCD}}^{\text{TH}}$.

Effects due to gluon splitting to $b\bar{b}$ and $c\bar{c}$ have been estimated by rescaling the JETSET simulation production of such quark pairs to current world-average gluon splitting measurements [15], leading to a correction of $+0.3\%$ on the value of A_b . Additional radiative effects, such as those due to initial-state radiation and γ/Z interference,

lead to a further correction of -0.2% to the measured value of A_b .

While, as described above, the overall tagging efficiency is derived from data, the dependence of the b -tagging efficiency upon the secondary vertex mass must be estimated from the MC simulation, as must be the charm correct-signing probability p_c . The value of A_c is set to its standard model value of 0.67, with an uncertainty commensurate with that of [16]. The value of $A_{b\text{ckg}}$ is set to zero, with an uncertainty corresponding to the full physical range $|A_{b\text{ckg}}| < 1$. The resulting value of A_b extracted from the fit is $A_b = 0.907 \pm 0.022(\text{stat})$. This result is found to be insensitive to the value of the b -tag mass cut, and the value of weighting exponent κ used in the definition (2) and (3) of the momentum-weighted track-charge sum.

We have investigated a number of systematic effects which can change the measured value of A_b ; these are summarized in Table I. The uncertainty in α_b due to the statistical uncertainties in $\langle |Q_{\text{dif}}|^2 \rangle$ and σ_{sum}^2 corresponds to a 1.6% uncertainty in A_b . The uncertainty in the hemisphere correlation parameter λ is estimated by varying fragmentation parameters within JETSET 7.4, and by comparison with the HERWIG 5.7 [18] fragmentation model. The resulting uncertainty in A_b is 1.4%. The sensitivity of the result to the shape of the underlying Q_b distribution is tested by generating various triangular distributions as well as double Gaussian distributions with offset means. The test distributions are constrained to yield a Q_{sum} distribution consistent with data, and the total uncertainty is found to be 0.8%. In addition, while the mean value of the self-calibration parameter α_b is constrained by the data, it has a $\cos\theta$ dependence due to the falloff of the tracking efficiency at high $|\cos\theta|$ which must be

TABLE I. Relative systematic errors on the measurement of A_b .

Error source	Variation	$\delta A_b/A_b$
<i>Self-calibration</i>		
α_b statistics	$\pm 1\sigma$	1.6%
λ_b correlation	JETSET, HERWIG	1.4%
$P(Q_b)$ shape	Different shapes	0.8%
$\cos\theta$ shape of α_b	MC shape vs flat	0.4%
Light flavor	50% of correction	0.2%
<i>Analysis</i>		
Tag composition	Procedure from [17]	0.5%
Detector modeling	Compare tracking efficiency corrections	0.8%
Beam polarization	$\pm 0.5\%$	0.5%
QCD	Full correction	0.3%
Gluon splitting	Full correction	0.1%
A_c	0.67 ± 0.04	0.1%
$A_{b\text{ckg}}$	0 ± 0.50	0.2%
Total		2.6%

estimated using the simulation, leading to a 0.4% uncertainty in A_b .

The extracted value of A_b is sensitive to our estimate of the $Z^0 \rightarrow c\bar{c}$ background, which tends to reduce the observed asymmetry due to the positive charge of the underlying c quark. The uncertainty in the purity estimate of $96.9\% \pm 0.3\%$ is dominated by the uncertainties in the charm tagging efficiency ($\epsilon_c = 0.0218 \pm 0.0004$) and the statistical uncertainty of the bottom tagging efficiency determined from data, leading to a 0.5% uncertainty in A_b . An outline of the charmed quark efficiency uncertainty determination can be found in Ref. [17]; the uncertainty is dominated by empirical constraints on charmed hadron production rates and on K^0 production in the decay of charmed mesons. Uncertainties in the measured values of R_b and R_c contribute, through the tag purity, to uncertainties in A_b of 0.1% and 0.0%, respectively.

Agreement between the data and MC simulation charged track multiplicity distributions is obtained only after the inclusion of additional *ad hoc* tracking inefficiency. This random inefficiency was parametrized as a function of total track momentum, and averages 0.4 charged tracks per event, leading to an overall change of +1.3% in A_b . As a check, we employ an alternative approach, matching the efficiency of the linking of the independent CDC and VXD3 track segments between data and MC simulation. This yields a change of +0.5% in A_b ; we take the difference of 0.8% as an estimate of the systematic error on the modeling of the tracking efficiency. Combining all systematic uncertainties in quadrature yields a total relative systematic uncertainty of 2.6%.

The extracted value of A_b depends on a number of model parameters, as follows. Increases by 0.01 in the values of A_c , R_b , R_c , and the per-event rate of $b\bar{b}$ production via gluon splitting lead to changes in A_b of +0.0002, -0.0055, +0.0002, and +0.0110, respectively.

In conclusion, we have exploited the highly polarized SLC electron beam and precise vertexing capabilities of the SLD detector to perform a direct measurement of $A_b = 0.906 \pm 0.022(\text{stat}) \pm 0.023(\text{syst})$, from the 1996–1998 SLD data sample. Combined with our previously published result [3] based on the 1993–1995 data sample, we find

$$A_b = 0.907 \pm 0.020(\text{stat}) \pm 0.024(\text{syst}), \quad (8)$$

for the full 1993–1998 data sample. This result is in good agreement with the standard model prediction of 0.935, and represents an improvement of over a factor of 2 in the

precision of the determination of A_b via the use of momentum-weighted track charge.

We thank the staff of the SLAC accelerator department for their outstanding efforts on our behalf. This work was supported by the U.S. Department of Energy and the National Science Foundation, the U.K. Particle Physics and Astronomy Research Council, the Istituto Nazionale di Fisica Nucleare of Italy, and the Japan-U.S. Cooperative Research Project on High Energy Physics. This work was supported in part by the Department of Energy Contract No. DE-AC03-76SF00515.

-
- [1] The LEP collaborations and the LEP electroweak working group, CERN Report No. CERN-EP-2001-021, 2001, and references therein.
 - [2] R. D. Field and R. P. Feynman, Nucl. Phys. **B136**, 1 (1978).
 - [3] K. Abe *et al.*, Phys. Rev. Lett. **81**, 942 (1998).
 - [4] K. Abe *et al.*, Phys. Rev. Lett. **78**, 2075 (1997).
 - [5] K. Abe *et al.*, Phys. Rev. D **53**, 1023 (1996); P. Rowson, D. Su, and S. Willocq, Annu. Rev. Nucl. Part. Sci. **51**, 345 (2001).
 - [6] K. Abe *et al.*, Phys. Rev. Lett. **84**, 5945 (2000).
 - [7] K. Abe *et al.*, Nucl. Instrum. Methods Phys. Res., Sect. A **400**, 287 (1997).
 - [8] G. Agnew *et al.*, SLAC Report No. SLAC-PUB-5906, 1992.
 - [9] W. Bartel *et al.*, Z. Phys. C **33**, 23 (1986).
 - [10] D. Jackson, Nucl. Instrum. Methods Phys. Res., Sect. A **388**, 247 (1997).
 - [11] K. Abe *et al.*, Phys. Rev. Lett. **74**, 2890 (1995).
 - [12] V.V. Serbo, Ph.D. thesis, University of Wisconsin (SLAC-REPORT-510, 1997).
 - [13] T. Sjöstrand *et al.*, Comput. Phys. Commun. **82**, 74 (1994).
 - [14] J. B. Stav and H. A. Olsen, Phys. Rev. D **52**, 1359 (1995); **50**, 6775 (1994); V. Ravindran and W. L. van Neerven, Phys. Lett. B **445**, 214 (1998); S. Catani and M. Seymour, J. High Energy Phys. 9907 (1999) 023; our implementation of these calculations is in accordance with CERN Report No. CERN-EP-2000-016, 2000, and references therein.
 - [15] K. Abe *et al.*, Phys. Lett. B **507**, 61 (2001); G. Abbiendi *et al.*, Eur. Phys. J. C **18**, 447 (2001); P. Abreu *et al.*, Phys. Lett. B **462**, 425 (1999); P. Abreu *et al.*, Phys. Lett. B **405**, 202 (1997); R. Barate *et al.*, Phys. Lett. B **434**, 437 (1998).
 - [16] LEP Electroweak Working Group, CERN Report No. CERN-EP-2000-16, 2000.
 - [17] K. Abe *et al.*, Phys. Rev. Lett. **80**, 660 (1998).
 - [18] G. Marchesini *et al.*, Comput. Phys. Commun. **67**, 465 (1992).